Engineered Science
DOI: https://dx.doi.org/10.30919/es1664

# Synergistic Effect of Co-Pyrolysis of Low-Grade Coal and Heavy Oil

N. U. Nurgaliyev,[1,2,*] Ye. K. Aibuldinov,[1] E. E. Kopishev,[3] Zh. B. Iskakova,[1] A. Kolpek,[3] A. S. Sabitov,[3,*] L. A. Kusepova,[3] R. M. Salikhov [4] and M. S. Petrov[4]

## Abstract

This study explores the co-pyrolysis of low-rank coal with heavy oil to address challenges in processing high-viscosity crude oil. Various coal-to-oil ratios were tested to evaluate yield and thermal behavior. Adding 20–80% heavy oil increased tar and gas yields by 50.69% and 10.39%, respectively, while reducing semi-coke yield by 61.08%. The presence of heavy oil lowered peak decomposition temperatures in DTG spectra and intensified corresponding peaks, indicating enhanced reactivity. A positive synergistic effect was observed at 80% oil addition, while 20–60% additions showed a negative effect. This synergistic effect was confirmed by TG-DTG-DSC analysis, revealing maximum weight loss and loss rates at 80% oil. Tar composition shifted, with a 20.64% rise in aromatic hydrocarbons and decreases in alkanes, olefins, and phenols by 9.76%, 2.44%, and 2.71%, respectively. Gas analysis showed increased $H_2$, $CH_4$, and $C_nH_m$, with lower CO and $CO_2$ levels, likely due to hydrogen from oil reacting with coal's oxygen groups via hydrogenolysis. These findings suggest that co-pyrolysis with heavy oil enhances product yield and quality, offering a promising route for upgrading heavy crude oil.

*Keywords:* Co-pyrolysis; Low-rank coal; Heavy oil; Synergistic effect; Pyrolysis tar; Gas composition; TG-DTG-DSC analysis; Aromatic hydrocarbons; Semi-coke; Hydrogen redistribution.
Received: 24 June 2025; Revised: 01 August 2025; Accepted: 01 August 2025
Article type: Research article.

## 1. Introduction

The coal industry of Kazakhstan is one of the most prominent sectors of the national economy. According to statistical data,[1] as of 2020, Kazakhstan ranked 10th globally in terms of coal reserves. However, a critical issue remains the practical utilisation of low-rank coal (LRC), which is limited due to its unfavourable characteristics. Low-rank coals, typically lignites or sub-bituminous coals, are characterised by low specific energy content due to their high moisture and/or ash content, as well as elevated emissions of harmful substances during combustion. In light of the increasing demand for electricity, the need to utilise such coal types is also growing.[2] Nonetheless, the direct application of these coals either leads to increased costs associated with emission control or reduces the efficiency of power generation systems, which in turn contributes to higher greenhouse gas emissions. Under current conditions, marked by restrictions on carbon emissions, it is essential to enhance the properties of low-rank coals in terms of moisture, ash content, and other trace elements.[2]

Pyrolysis of LRC is regarded as an optimal method for clean and efficient production of blue coke, tar, and gas.[3] Among the valuable products derived from coal, tar is the principal output of pyrolysis and can serve as an important feedstock for the production of olefins,[4,5] value-added aromatic compounds,[6] and coal tar-based materials.[4]

To improve the efficiency of the pyrolysis process and simultaneously involve various other types of waste, numerous researchers around the world have conducted studies on the co-pyrolysis of coal with different additives. In experimental studies, the following types of waste, primarily biomass, were used as additives: elm sawdust,[7] corn stover,[8] elm;[9] raw/torrefied biomass;[10] sugarcane bagasse, corn residues, and corn stover;[11] sugarcane bagasse;[12] palm kernel shell;[13] spent coffee grounds and waste rubber granulate;[14] pine sawdust;[15] microalgae biomass;[16] wheat straw, walnut shell, and wood chips;[17] plastic waste;[18,19] and waste tires.[20,21] Review studies have also been conducted, focusing on microwave pyrolysis of coal and biomass for fuel production,[22] and on investigating the properties of co-pyrolysis char derived from coal mixed with biomass.[23]

[1]*Research Institute of New Chemical Technologies, L.N. Gumilyov Eurasian National University, Astana, 010008, Kazakhstan*
[2]*Department of Chemistry, Chemical Technology and Ecology, Kazakh University of Technology and Business named after K. Kulazhanov, Astana, 010000, Kazakhstan*

These co-pyrolysis studies primarily aim to optimise the yield and quality of pyrolysis products while also examining the synergistic effects that may arise during co-pyrolysis. The diverse characteristics of feedstock during co-processing can influence the reactivity and thermal behaviour of the samples and their products, and the synergistic effect can improve the quality of the resulting output.[24] Moreover, the co-pyrolysis of LRC with various feedstocks can enhance the coal conversion rate and utilisation rate.[16] In addition, co-pyrolysis is increasingly recognised not only for its potential to increase tar yield but also for reducing $NO_x$, $SO_x$, and volatile organic compound emissions.[17]

The synergistic effect of co-pyrolysis between LRC and biomass becomes more pronounced with decreasing coal rank, possibly due to the original structure of low-rank coals, which includes large pores and small clusters of aromatic structures that are readily preserved as tar during rapid co-pyrolysis.[25] In the co-pyrolysis of LRC and biomass (apple branch), a synergistic effect was observed, which facilitated an increase in monocyclic and bicyclic aromatic hydrocarbons.[26] The proportion of aromatic hydrocarbons and phenols rose significantly compared to theoretical values, while the C<10 fraction reached 86.48%, far exceeding the theoretical value of 12.68%. Co-pyrolysis of lignite and rice husk resulted in greater water production and lower tar yields.[27] The addition of rice husk led to a higher atomic C/H ratio in the resulting char due to polycondensation reactions that produced more condensed char. A synergistic effect was also reported for co-pyrolysis of bituminous coal and biomass, particularly at a mixing ratio of 70:30 (wt./wt.), 600 °C, and 0.3 MPa.[28] Tar yields were approximately 7.2% higher than those predicted by the theoretical sum of individual pyrolysis results, while char yields were approximately 4.5% lower. Additionally, the content of phenolic compounds, aromatic hydrocarbons, and aliphatic hydrocarbons increased.

The results of co-pyrolysis involving low-rank pulverised coal and direct coal liquefaction residue (DCLR) demonstrated a significant synergistic effect.[29] Both feedstocks acted as hydrogen donors, thereby promoting the hydrogenation of small molecular radical fragments, which led to a 5.55% increase in tar yield. Within the resulting tar, the content of alkanes increased by 12.25%, while the levels of aromatic hydrocarbons and phenols decreased by 11.88% and 7.94%, respectively. The methane ($CH_4$) content in the gas phase rose by 19.60%, whereas the hydrogen ($H_2$) content decreased by 19.05%. A synergistic effect was also observed when DCLR was added to lignite; the actual yield of pyrolytic char exceeded the theoretical value with increasing DCLR dosage. This, in turn, resulted in highly aromatic and more ordered char structures, while the porous structure of the coal became less developed.[30]

The synergistic interaction between LRC and DCLR enhances the reactivity of radical fragments, thereby increasing tar yield during pyrolysis.[31] Maximum tar and hydrogen yields of 22.79% and 37.12%, respectively, were achieved at a DCLR addition of 40%. When 60% DCLR was used, the minimum semi-coke yield was recorded at 65.01%, and the maximum gas yield reached 14.65%. A pronounced synergistic effect was also observed during the co-pyrolysis of LRC and coking coal, where the latter's addition increased the formation of colloidal structures and facilitated interactions among pyrolysis products.[32] Both coals served as hydrogen donors; [H] radicals and fragments generated during pyrolysis promoted hydrogenation reactions.

In studies examining the co-pyrolysis of various coal grades and oil shale, synergy was also detected, where coal provided hydrogen to the shale, resulting in increased tar yields and the formation of high-value-added tar components.[33]

Another promising hydrocarbon feedstock for co-pyrolysis with LRC to produce high-value-added products is so-called "unconventional hydrocarbon feedstock", such as heavy (high-viscosity) crude oil and natural bitumen. This is due to the fact that the majority of the global growth in proven hydrocarbon reserves is attributed to these sources. For instance, heavy oil and natural bitumen are characterised by high contents of aromatic hydrocarbons, resinous-asphaltene substances, elevated concentrations of metals and sulfur compounds, as well as high density, viscosity, and coking potential. However, processing such feedstocks requires more complex technologies and greater financial and energy inputs compared to conventional hydrocarbon sources. On the other hand, due to its complex composition and high density and viscosity, heavy oil can infiltrate the pores of coal particles during thermal decomposition, coating them and increasing the contact surface area. This intimate contact can facilitate more efficient interactions between coal and oil particles.

Accordingly, the aim of the present study is to investigate the influence of various heavy oil additives on the co-pyrolysis process with low-rank coal, as well as to analyse the yield and characteristics of the resulting pyrolysis products. To identify and evaluate the synergistic effect between coal and oil, a thermal method (TG-DTA/DSC) was employed, enabling rapid acquisition of extensive information on the decomposition behaviour of the samples, with the registration of all transformation stages across a wide temperature range.[34]

## 2. Materials and methods

### 2.1 Materials

In this study, a low-rank coal of the long-flame type was utilised. The coal was sampled from the "Borly" coal deposit (Kazakhstan) and represents high-ash coal waste, predominantly consisting of fine coal particles with sizes

[3]*Department of Chemistry, Faculty of Natural Sciences, L.N. Gumilyov Eurasian National University, Astana, 010008, Kazakhstan*
[4]*LLC "TTU LTD", St. Petersburg, Russian Federation*
[*]*Email*-nurken.nu28@gmail.com (N. U. Nurgaliyev),
sabitov_as_1@enu.kz (A. S. Sabitov)

**Table 1:** Characteristics of the Raw Feedstocks.

| Sample | Proximate analysis (wt.%) | | | | Ultimate analysis (wt.%) | | | | | Molar ratio | |
|---|---|---|---|---|---|---|---|---|---|---|---|
| | M | A | V | FC | C | H | O* | N | S | H/C | O/C |
| coal | 5.34 | 47.38 | 22.31 | 24.97 | 84.41 | 5.96 | 6.94 | 1.19 | 1.50 | 0.84 | 0.06 |
| oil | 6.59 | 0.10 | 90.94 | 2.37 | 83.75 | 10.08 | 3.96 | 0.52 | 1.69 | 1.43 | 0.04 |

M: moisture; A: Ash content; V: Volatile matters; FC: Fixed carbon; O*: Oxygen (by difference); N: Nitrogen; S: Sulfur.

below 5 mm. After grinding in a ball mill, the coal was sieved to achieve a particle size of less than 200 μm and subsequently dried for further use. Samples of heavy (high-viscosity) crude oil were collected from the "Sarybulak" oil and gas field (Zaysan Basin, Kazakhstan). Composite representative samples of both types of raw materials were prepared in advance.

Table 1 presents the elemental composition of the coal and oil. As shown, the coal is characterised by extremely high ash content (47.38%), low volatile matter (22.31%). In contrast to coal, the high-viscosity oil exhibits very low ash content (0.10%) and significantly higher values of volatile matter (90.94%) as well as carbon and hydrogen contents. The hydrogen content in the oil is about 10%, which is favourable for improving the quality of the pyrolysis products due to hydrogen redistribution and the formation of a large number of active hydrogen radicals.[35] Furthermore, the higher H/C ratio of the oil (compared to coal) indicates a predominance of alkanes and olefins in the oil, while the higher O/C ratio of the coal suggests a greater presence of oxygen-containing compounds such as aromatic hydrocarbons, phenols, ketones, and aldehydes.

To carry out co-pyrolysis of low-rank coal with heavy oil, samples were prepared at different additions of oil to coal (from 20% to 80%), *i.e.* at mass ratios of coal and oil being 100/0, 80/20, 60/40, 40/60, 20/80, 0/100, respectively.

### 2.2 Experimental procedure

The samples were air-dried until an approximate equilibrium was achieved between the sample moisture content and the ambient atmosphere. The coal and oil were thoroughly mixed by mechanical stirring to ensure homogeneous distribution of oil over the coal particles. A sample portion of 50 g was placed into an aluminium retort and heated under a nitrogen atmosphere (flow rate: 100 mL/min) at a heating rate of 10 °C/min up to 500 °C, with an isothermal hold at the final temperature for 90 minutes. The decomposition products were directed into a condenser cooled with an ice–water mixture, where tar and water were condensed. The gaseous products, after sampling for analysis, were vented to the atmosphere.

Following pyrolysis, the yield of the liquid product and the solid residue was determined gravimetrically, while the yield of pyrolysis gas was calculated by mass balance, *i.e.* by subtracting the mass of the liquid product and solid residue from the initial sample mass. All experiments were performed in triplicate, and average values were reported.

### 2.3 Analysis and characterization

The proximate analysis data presented in Table 1 were obtained experimentally using a LABSYS Evo TG-DTA/DSC instrument (SETARAM, France) in accordance with ASTM D7582-12 "Standard Test Methods for Proximate Analysis of Coal and Coke by Macro Thermogravimetric Analysis." The measurements included moisture, volatile matter, ash, and fixed carbon content.

The ultimate (elemental) analysis of coal and oil was performed using a Flash EA 1112 elemental analyzer (Thermo Fisher Scientific, USA). This analysis determined the content of carbon, hydrogen, nitrogen, and sulfur. Oxygen was calculated by difference.

All results presented in Table 1 are original experimental data and not derived from literature sources.

To investigate the thermal behaviour of the samples during pyrolysis, thermal analysis was performed using a LABSYS Evo TG-DTA/DSC instrument (SETARAM, France), which enables simultaneous thermal analysis. This model allows for the concurrent measurement of thermogravimetric analysis (TG), differential thermal analysis (DTA), and differential scanning calorimetry (DSC). The analysis was conducted on approximately 5 mg of sample over a temperature range from ambient to 1000 °C, at a heating rate of 20 °C/min. Nitrogen was used as the carrier gas to maintain an inert atmosphere. The nitrogen volume flow rate was 60 mL/min.

Thermal decomposition parameters such as Tonset, Tmax, DTGmax, and weight loss were extracted using the manufacturer's integrated analysis software (SetSoft 2000).

Elemental composition (Table 1, ultimate analysis) of the raw materials was determined using an automated elemental analyser (Flash EA 1112). The pyrolysis tar composition was analyzed using a GC–MS system (GCMS-QP2010 Plus, Shimadzu) equipped with a DB-5 capillary column (60 m length, 0.25 mm inner diameter, 0.25 μm film thickness). High-purity helium (99.999%) was used as the carrier gas at a flow rate of 1 mL/min. Ionization was performed by electron impact at 70 eV. The injector (TINJ) and detector (TDET) temperatures were both maintained at 300 °C. A splitless injection mode was employed with an injection volume of 1 μL. Data processing was carried out using GCMS solution software. The liquid samples were analyzed directly, without

derivatization. Infrared spectroscopy of the pyrolytic char was conducted using a Fourier-transform infrared (FTIR)spectrometer Shimadzu IRTracer-100, equipped with an ATR-8000A accessory featuring a diamond crystal. The composition of the gaseous products obtained from coal and oil pyrolysis was determined by gas adsorption chromatography using a Crystallux 4000M chromatograph (Meta-Chrom, Russia), equipped with a thermal conductivity detector: Hayesep R packing column (80/100 mesh) (length - 3 m, diameter – 3 mm ), NaX packing column (60/80 mesh) (length -3 m, diameter – 3 mm), detector – flame ionisation, carrier gas – helium. Column temperature regime – isothermal at 90 °C, helium flow rate 30 ml/min. Detector temperature – 210 °C, evaporator temperature – 150 °C.

### 2.4 Calculation of theoretical values

To investigate the interaction between coal and oil during the co-pyrolysis process, the experimental yields of pyrolysis products (tar, gas, and semi-coke) and the mass loss of the samples (as observed through TG-DTG-DSC analysis) were compared with calculated (theoretical) values. The latter were determined based on the assumption of no interaction between coal and oil, using a weighted average approach according to Eq. (1)[36] and (2).[37]

The theoretical yields of individual pyrolysis products during co-pyrolysis ($Y_{cal,i}$) were calculated using the following weighted average equation:

$$Y_{cal,i} = (1 - x)\, Y_{coal,i} + x Y_{oil,i} \quad (1)$$

where *i* denotes the type of pyrolysis product (tar, gas, or semi-coke); $Y_{cal,i}$ is the calculated yield of product *i* during co-pyrolysis; $Y_{coal,i}$ and $Y_{oil,i}$ are the experimentally measured yields of product *i* from coal and oil, respectively; and *x* is the mass fraction of oil in the mixture.

The theoretical mass loss ($Z_{cal}$) during co-pyrolysis was determined using Eq. (2):

$$Z_{cal} = xZ_{coal} + yZ_{oil} \quad (2)$$

where $Z_{coal}$ and $Z_{oil}$ represent the experimental mass loss values for coal and oil, respectively, obtained from individual pyrolysis. *x* and *y* are the mass fractions of oil and coal in the mixture, respectively.

## 3. Results and discussion

### 3.1 Yields of pyrolysis products

The results of the co-pyrolysis process of low-rank coal and heavy oil are presented in Fig. 1. The addition of oil in proportions ranging from 20% to 80% led to favourable co-pyrolysis performance, as evidenced by a substantial increase in tar yield (from 16.34% to 67.03%) and gas yield (from 6.15 % to 16.54%), as well as a significant reduction in semi-coke yield (from 77.51% to 16.43%). For incremental oil additions of 0–20%, 20–40%, 40–60%, and 60–80%, the tar yield increased by 8.49%, 14.93%, 9.02%, and 26.74%, respectively. This increase in tar and gas yields is presumably due to the high content of heavy hydrocarbons in the oil (*e.g.*, resins and asphaltenes), which generate reactive free radicals upon heating, thus promoting the thermal decomposition of coal and favoring liquid and gas formation. The free radicals generated during the co-pyrolysis process accelerate the thermal decomposition of coal by facilitating the cleavage of strong carbon–carbon (C–C) and carbon–hydrogen (C–H) bonds within the coal matrix. Moreover, the higher content of hydrogen-rich compounds in the oil-particularly its naphthenic and paraffinic fractions-promotes the formation of liquid products while simultaneously suppressing the generation of semi-coke.

The above-mentioned processes that contribute to the increased formation of liquid and gaseous products may hypothetically correspond to the following key chemical reactions (R – hydrocarbon group; R• – hydrocarbon radical; H – hydrogen radical; Ar – aromatic group):

1. Cracking of heavy oil fractions (resulting in lower molecular weight liquid and gaseous products):

- $R–CH_2–CH_2–CH_2–R' \rightarrow R–CH_2• + •CH_2–CH_2–R'$ (homolytic cleavage of C–C bonds forming hydrocarbon radicals);
- $R–CH_2–CH_3 \rightarrow R–CH_2• + •CH_3$ (homolytic cleavage of C–C bond in alkyl side chains);
- $R–CH_3 \rightarrow R• + •CH_3$ (thermal radical cleavage of methyl groups);
- $R–CH_2–CH_2–CH_3 \rightarrow R–CH_3 + CH_2=CH_2$;
- $R–CH_2–CH_2–CH_3 \rightarrow R–CH_3• + CH_2=CH_2 + H•$ (radical cracking with ethylene formation);
- $R–CH_2–CH_2–R \rightarrow R–CH_2• + •CH_2–R$ (radical cracking of alkanes);
- $R–CH_2–CH_2–CH_2–R' \rightarrow R–CH=CH_2 + R'–CH_3$;$R–CH_2–CH_2–CH_2–CH_3 \rightarrow R–CH_3 + CH_2=CH–CH_3$ (cracking with alkene and alkane formation);
- $Ar–CH_2–CH_2–OH \rightarrow Ar–CH=CH_2 + H_2O$ (thermal dehydration of aromatic alcohol);
- $R–COOH \rightarrow R–H + CO_2$ (decarboxylation of carboxylic acid);
- $R–CHO \rightarrow R–H + CO$ (decarbonylation of aldehyde);
- $Ar–R–R' \rightarrow Ar–R• + R'•$ (radical cleavage of side chains in aromatic hydrocarbons);
- $R–CH_2–CH_3 \rightarrow R–CH=CH_2 + H_2$ (dehydrogenation of ethyl side chains forming vinyl groups);
- $CH_3–CH_2–R \rightarrow CH_2=CH–R + H_2$ (dehydrogenation of

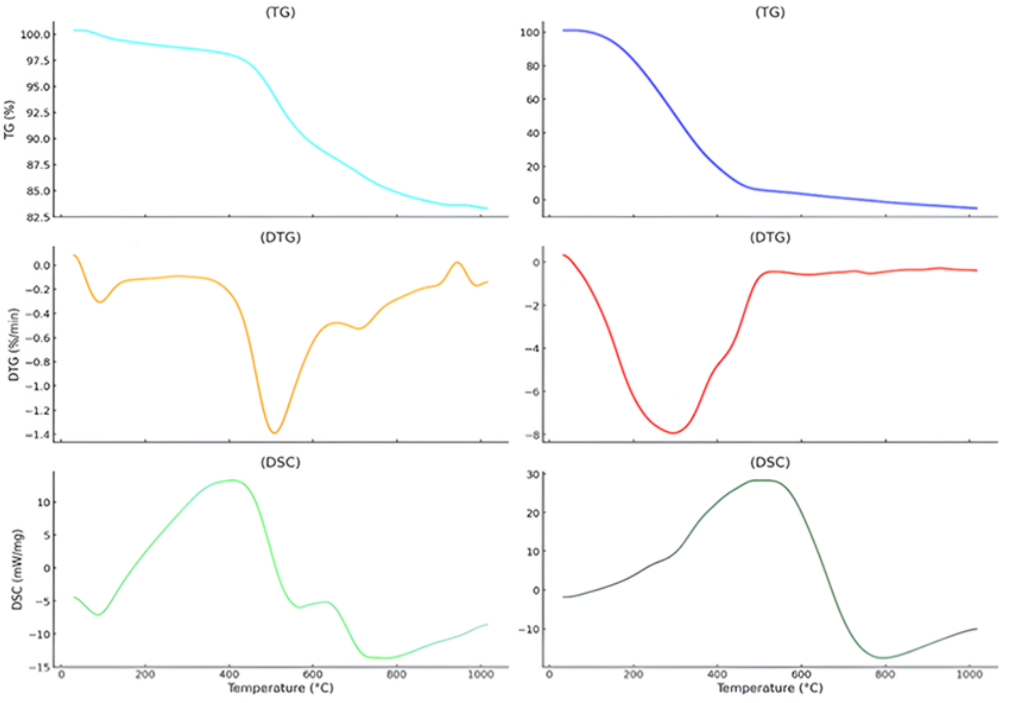


**Fig. 1:** Effect of Various Oil Additions (0–100%) on the Experimental (solid line) and Theoretical (dashed line) Yields of Co-Pyrolysis Products with Coal.

linear alkanes forming α-olefins).

2. Initiation of coal pyrolysis by oil-derived radicals:

- Ar– $CH_2$–Ar′ + R• → Ar–CH•–Ar′ + RH (cleavage of methylene bridges between aromatic coal structures by oil radicals);
- Ar–H + R• → Ar• + RH (hydrogen abstraction from aromatic coal fragments);
- R• (from oil) + Ar– $CH_2$– $CH_2$–Ar → R–$CH_2$–$CH_2$–Ar + Ar• (radical transfer activating aromatic structures in coal);
- $CH_3$• + Ar–OH → $CH_4$ + ArO• (hydrogen transfer from phenol to methyl radical).

3. Hydrogenation of coal radicals by hydrogen-containing compounds in oil:

- $C_5H_{10}$ → $C_5H_9$• + H• (decomposition of naphthenes producing hydrogen radicals);
- Ar• + H• → Ar–H (stabilization of coal radicals);
- R• + H• → RH (stabilization of hydrocarbon radicals forming liquid fractions);
- Ar• + $CH_4$ → Ar–H + $CH_3$• (hydrogenation of aromatic radicals forming stable Ar–H structures);
- Ar• + R–$CH_3$ → Ar–H + R–$CH_2$• (hydrogen transfer from oil alkyl groups to coal radicals);
- $CH_3$• + H• → $CH_4$ (radical methanation).

4. Accelerated thermal decomposition of coal functional groups:

- Ar–COOH → Ar–H + $CO_2$ (decarboxylation with $CO_2$ release);
- Ar–CHO → Ar–H + CO (decarbonylation with CO release);
- Ar–$CH_2$–OH → Ar–H +
- $CH_2O$ (cleavage of hydroxymethyl groups forming formaldehyde);
- Ar–CO–$CH_3$ → Ar• + $CH_3$• + CO (thermal radical decarbonylation of ketones).

5. Alkylation of aromatic coal structures by oil-derived radicals:

- Ar• + $CH_3$• → Ar– $CH_3$ (radical recombination forming alkyl-substituted aromatics);
- Ar–H + $CH_3$• → Ar– $CH_3$+ H• (radical alkylation of aromatic rings by methyl radicals);
- Ar–H + R• → Ar–R + H• (*e.g.*, Ar–H + $C_2H_5$• → Ar– $C_2H_5$ +H•) (radical alkylation forming liquid products such as alkylbenzenes—toluene, ethylbenzene, etc.).

A comparable effect of adding heavy oil to low-rank coal at a coal-to-oil ratio of 8:2 was observed in,[38] where tar and gas yields increased by 12.18% and 7.74%, respectively, while the solid residue yield decreased by 20%.

A comparison of experimental and theoretical yields of pyrolysis products revealed that only at an 80% oil addition did the experimental yields of tar and gas exceed their respective theoretical values, indicating the occurrence of a positive synergistic effect between coal and oil. In contrast, oil additions in the range of 20% to 60% resulted in experimental yields that were either lower than or approximately equal to

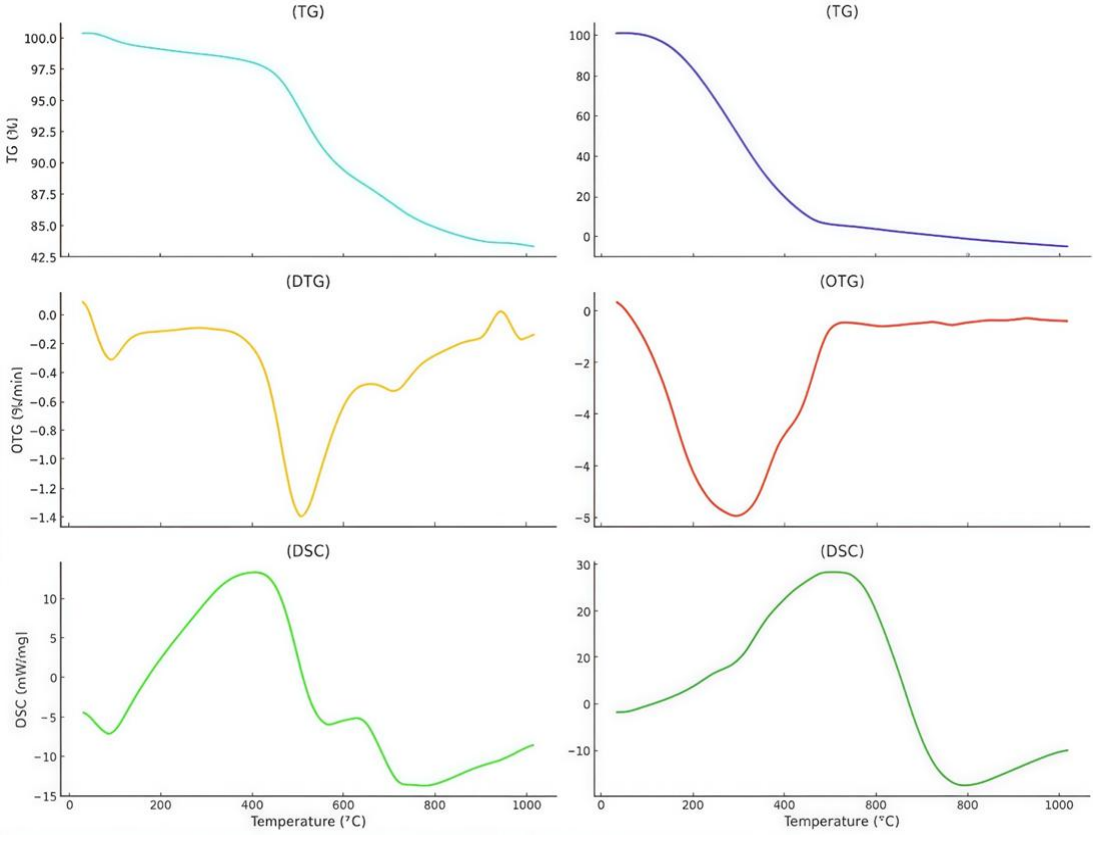


**Fig. 2:** TG/DTG/DSC Curves of Coal (A) and Oil (B) Samples.

the theoretical values, suggesting a negative synergistic effect The observed positive synergistic effect is presumably attributable to the significant differences in the properties of the coal and oil feedstocks. This is further supported by findings reported in,[39] where it is noted that varying chemical and physical characteristics of different feedstocks can lead to synergistic interactions. For instance, during the co-pyrolysis of biomass waste and oil sludge, the synergistic effect resulted in an increase in oil yield and improvement in its quality, due to an elevated H/C ratio (from 1.5 to 2.0) and an increase in higher heating value (from 19.5 to 24.5 MJ/kg).[26]

Thus, the optimal coal-to-oil ratio appears to be 20:80, which may be explained by several factors. At high oil content, the number of radicals formed from oil decomposition becomes sufficient to actively interact with coal macromolecules, disrupting their structure and enhancing the release of volatile matter. Moreover, the high concentration of hydrogen-rich compounds in the oil helps to stabilise the coal-derived radicals effectively.

In contrast, at lower oil content (20–60%), coal undergoes less extensive degradation, and the reactions are primarily governed by dehydrogenation and polymerisation processes within the coal matrix, thereby limiting the yields of liquid products and gases. Insufficient hydrogen-donating compounds at these lower oil ratios also result in more intense coke formation, with resinous intermediates undergoing secondary polymerization.

Overall, at higher oil contents, oil droplets more thoroughly coat the coal particle surfaces, increasing coal porosity and improving heat transfer. These effects collectively promote greater liquefaction of the coal matrix and substantially enhance tar and gas yields.

### 3.2 TG-DTG analysis

To confirm the presence of a synergistic effect between coal and oil during co-pyrolysis, a series of TG-DTG-DSC experiments was conducted. The TG-DTG-DSC curves obtained from the pyrolysis of coal, oil, and their mixtures are presented in Fig. 2 and 3. Based on these curves, the key thermal parameters at different coal-to-oil mass ratios are The observed decrease in the temperature at which pyrolysis summarised in Table 2 begins when heavy oil is added up to 40% (Table 2) can be explained by the fact that light oil fractions begin to thermally decompose at relatively low temperatures (up to ~200°C), forming active radicals that initiate coal pyrolysis and accelerate its decomposition. In addition, the presence of oil in the pores of coal particles improves heat transfer and reduces the strength of bonds, which also lowers the energy barrier for the reaction to start. A further increase in oil content from 40 to 80% leads to an increase in the pyrolysis start temperature, which may be associated with an increase in the total proportion of medium- and high-boiling fractions in the coal-oil mixture, whose evaporation temperature exceeds 200°C. At an oil content of

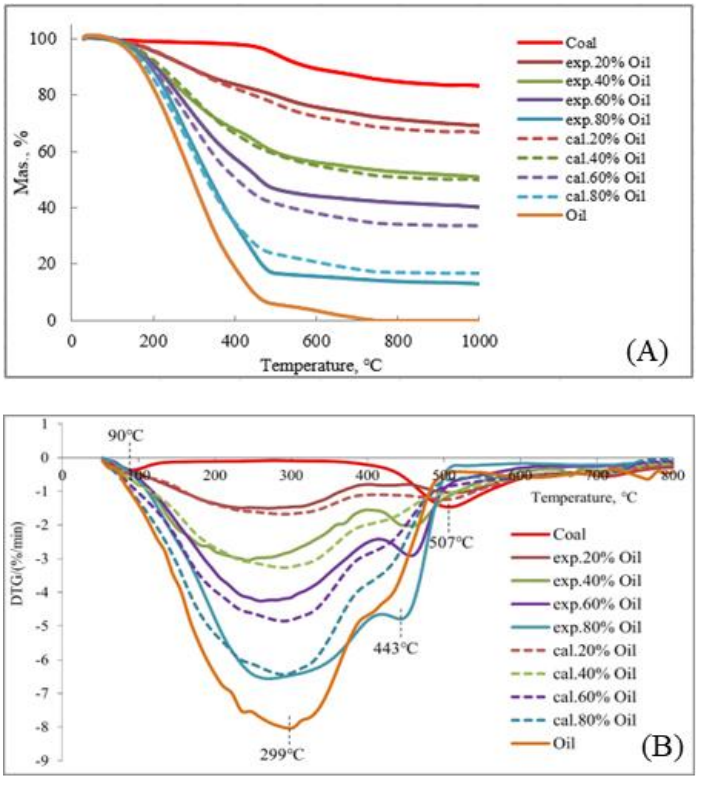


**Fig. 3:** Experimental and Theoretical TG (A) and DTG (B) Curves of Coal, Oil, and Coal-Oil Mixtures.

**Table 2:** Pyrolysis Characteristic Parameters at Different Oil Addition Levels.

| Oil Content (wt%) | $T_{onset}$ (°C) | $T_{1max}$ (°C) / $DTG_{1max}$ (%·min$^{-1}$) | $T_{2max}$ (°C) / $DTG_{2max}$ (%·min$^{-1}$) | $T_{3max}$ (°C) / $DTG_{3max}$ (%·min$^{-1}$) | $T_{end}$ (°C) | Weight loss (wt%) |
|---|---|---|---|---|---|---|
| 0 | 436.03 | – | 506.83 / 1.47 | 712.84 / 0.55 | 846.79 | 16.65 |
| 20 | 140.57 | 270.43 / 1.50 | 511.01 / 1.04 | 712.83 / 0.54 | 779.47 | 30.90 |
| 40 | 127.40 | 243.37 / 3.05 | 457.93 / 2.02 | 666.11 / 0.54 | 773.18 | 49.27 |
| 60 | 165.67 | 261.03 / 4.26 | 456.91 / 2.91 | – | 769.15 | 59.80 |
| 80 | 170.36 | 271.48 / 6.56 | 443.28 / 4.79 | – | 763.84 | 86.87 |
| 100 | 159.76 | 299.43/ 8.04 | – | – | 721.16 | 97.72 |

$T_{onset}$ − onset temperature of pyrolysis, $T_{1max}$, $T_{2max}$, $T_{3max}$ −temperature at which the maximum weight loss rate is reached within a specific temperature range, $T_{end}$ − final temperature of the pyrolysis process.

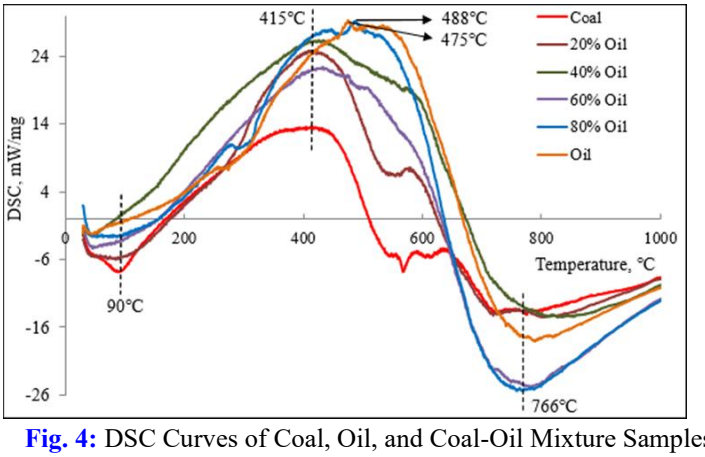


**Fig. 4:** DSC Curves of Coal, Oil, and Coal-Oil Mixture Samples.

100%, the pyrolysis start temperature decreases again, which is apparently due to the absence of the solid phase of coal, since it is precisely this phase that can create diffusion and thermal barriers in mixed systems and requires additional energy to heat up and break the strong chemical bonds in its structure.

Analysis of the obtained data revealed that oil additions in the range of 20–80% led to a significant increase in sample weight loss (approximately from 17% to 87%). Notably, the highest weight loss was observed at 80% oil addition, compared to other oil additions (20–60%). This is clearly illustrated in the TG and DTG spectra (Fig. 3), as well as in Table 2, which summarises the $DTG_{max}$ values and total weight loss during pyrolysis. For example, the weight loss difference between 60% and 80% oil addition was 27.07%, the largest among all tested compositions. Moreover, comparative analysis of the experimental and theoretical data showed that only at 80% oil addition were the experimental TG-DTG curves situated below the theoretical ones (Fig. 3), indicating a positive synergistic effect. In contrast, at oil additions of 20–60%, the experimental curves lay above the theoretical ones, indicating a negative synergistic effect.

The DTG curve of 100% coal exhibited three main decomposition stages, with peak weight loss rates occurring at 90.06, 506.83, and 712.84 °C. These values are consistent with data reported for other types of coal.[35,38,40,41] The small peak at 90.06 °C on the DTG curve reflects a slow weight loss rate and is attributed to the release of physically adsorbed moisture from the raw sample.[41] The addition of 20% oil caused this initial peak to broaden and gave rise to a new major peak that was not observed in 100% coal. With further oil addition, this peak became more prominent, appearing within a narrow range of 270–299 °C, and was the most intense among the three. This first decomposition stage is likely associated with the release of low-boiling-point compounds (present in the oil), the cleavage of weak chemical bonds, and recombination reactions with the release of $CO_2$ and light volatile compounds.[38]

As the temperature increased, the second decomposition stage occurred. Here, the peak weight loss temperature shifted to lower values (from approximately 507 °C to 443 °C), and for 100% oil, this peak was completely absent. This stage corresponds to the intense breakdown of stronger chemical bonds in the organic matter of coal and oil, particularly oxygen-containing functional groups, resulting in the formation of significant amounts of gas. During this stage, depolymerisation and decomposition of coal and oil structures occur, forming semi-coke, and radical fragments produced by bond cleavage interact with active hydrogen atoms to generate large quantities of volatiles and tar.[40]

At temperatures exceeding 650 °C, the third decomposition stage was observed. Similar to the second peak, the third DTG peak also shifted to lower temperatures (from 713 °C to 666 °C) with increasing oil content, and disappeared completely at oil additions of 60% and 80%. This stage may involve condensation and carbonisation reactions leading to the formation of coke, alongside the release of small amounts of gaseous products. The disappearance of the second and third peaks may be attributed to the accelerating effect of high oil additions, which promote early release of most volatiles before reaching $T_{2max}$ and $T_{3max}$.

The DSC curve of the coal sample exhibited an endothermic peak at 90 °C, attributed to heat absorption during the removal of physically adsorbed moisture, which is consistent with the DTG curve (Fig. 4). In all DSC spectra, two major thermal events were identified: an exothermic peak in the range of 415–488 °C and an endothermic peak around 766 °C. The first peak was significantly more intense, as it corresponds to primary thermal processes such as the decomposition of organic matter, dehydrogenation, and the formation of semi-coke. The second peak is mainly associated with the release of residual volatiles and coke formation.

The addition of oil led to a substantial increase in the intensity of the exothermic peak compared to the coal alone, due to the higher content of volatile compounds and more intense hydrocarbon decomposition. At 80% oil content, not only was the peak intensity markedly enhanced, but the exothermic peak also shifted to a considerably higher temperature, closely resembling the thermal behavior of pure oil—further confirming the presence of a synergistic interaction between coal and oil.

### 3.3 Results of the component analysis of pyrolysis tar

Table 3 presents the component composition of tar obtained from the pyrolysis of coal, oil, and a coal–oil mixture at the optimal ratio of 20:80. The results of the pyrolysis tar analysis showed that the tar derived from coal and oil primarily consisted of alkanes, olefins, aromatic hydrocarbons, and phenols. Small quantities of alcohols, ketones, and aldehydes were also detected.

The high content of aromatic hydrocarbons in coal-derived tar (50.27%) may be attributed to the development of polycyclic structures and dehydration of the coal matrix during pyrolysis. The relatively high amount of phenolic compounds (15.37%) is likely due to the cleavage of oxygen-containing functional groups throughout the pyrolysis process.

In contrast, the high alkane content in oil-derived tar (31.82%) suggests a low degree of aromatisation, while the low phenol content (5.18%) may be related to the limited presence of heteroatoms in the original oil feedstock.

The theoretical percentage content of the components in the pyrolysis tar was calculated using the following Eq. (3):

$$W_{cal} = 0.2W_{coal} + 0.8W_{oil}, \quad (3)$$

where $W_{coal}$ (%) is the percentage content of a given component in the tar derived from coal pyrolysis, and. $W_{oil}$ (%) is the corresponding value from oil pyrolysis.

Comparative analysis of the theoretical and experimental data revealed a substantial increase in the content of aromatic hydrocarbons (by 20.64%) and a noticeable reduction in

**Table 3:** Component Composition of Pyrolysis Tar.

| Sample | Components, wt% | | | | | | |
|---|---|---|---|---|---|---|---|
| | Alkanes | Olefins | Aromatic Hydrocarbons | Phenols | Alcohols | Ketones | Aldehydes |
| Coal | 12.45 | 3.18 | 50.27 | 15.37 | 1.51 | 1.74 | 1.64 |
| Oil | 31.82 | 8.42 | 37.25 | 5.18 | 2.26 | 0.53 | 0.83 |
| Coal + Oil (20/80) | 18.19 | 4.93 | 60.49 | 4.51 | 1.54 | 1.58 | 1.96 |
| Theoretical value | 27.95 | 7.37 | 39.85 | 7.22 | 2.11 | 0.77 | 0.99 |

alkanes (by 9.76%), as well as slight decreases in olefins (by 2.44%) and phenols (by 2.71%). The significant increase in aromatic hydrocarbons can be attributed to the dehydrogenation and dehydrocyclization of long-chain alkanes and alkyl-aromatic compounds in heavy oil, as shown in Eq. (4-6).

$$C_nH_{2n+2} \rightarrow C_nH_{2n} + H_2 \quad \text{(dehydrogenation of alkanes)} \quad (4)$$

$$C_nH_{2n} \rightarrow C_nH_{2n-2} + H_2 \quad \text{(dehydrocyclisation of alkenes)} \quad (5)$$

$$C_nH_{2n-2} \rightarrow \text{aromatic hydrocarbons} + H_2 \quad \text{(formation of benzene rings)} \quad (6)$$

Moreover, the high concentration of hydrocarbon radicals in the mixture promotes radical condensation reactions, leading to the formation of polycyclic aromatic hydrocarbons, for example, through benzene condensation into polyaromatic compounds such as naphthalene, with hydrogen release. The decrease in alkane content may be attributed to their thermal decomposition into short-chain radicals, which subsequently undergo secondary aromatisation, as shown in Eq. (7-8).

$$R - CH_3 \rightarrow R\bullet + CH_4 \text{ (homolytic bond cleavage)}, \quad (7)$$

$$R\bullet + H\bullet \rightarrow R - H \text{ (radical hydrogenation)} \quad (8)$$

In the presence of coal-derived radicals, active hydrogen atom redistribution occurs, facilitating the breakdown of saturated chains and thereby reducing the alkane content in the tar.

Since phenols predominantly originate from oxygen-containing functional groups, their decreased content may be attributed to the relatively small proportion of coal (20%) in the blend. Furthermore, the high concentration of hydrogen radicals generated from the oil may promote the hydrogenation of phenolic groups to hydrocarbons, as shown in Eq. (9).

$$C_6H_5OH + H_2 \rightarrow C_6H_6 + H_2O \quad \text{(hydrogenation of phenol to benzene)} \quad (9)$$

Phenols may also be converted into cyclitols, which can further decompose into light gaseous hydrocarbons and $H_2O$.[38] Meanwhile, the contents of alcohols, ketones, and aldehydes remained nearly unchanged, likely due to their lower susceptibility to secondary transformations.

Table 4 shows that the contents of the light and heavy fractions in coal-derived tar are 44.61% and 13.59%, respectively, which contrasts significantly with the corresponding values in oil-derived tar-15.17% and 36.07%, respectively. This difference directly influenced the distribution of light and heavy fractions in the tar obtained from the coal–oil mixture. Compared to the theoretical values, the content of the light fraction in the mixed tar decreased by 7.53%, while the medium and heavy fractions increased by 4.86% and 7.55%, respectively.

The reduction in the light fraction may be attributed to the hydrogenation of light hydrocarbons (present in oil), followed by their cracking into low-molecular-weight gases and $H_2O$. It may also result from the aromatisation of light alkanes and olefins (from oil) into higher molecular weight aromatic compounds. Conversely, the increase in medium and heavy fractions may be associated with the hydrogenolytic cracking of the heavy fraction in the oil and the inhibition of cracking of high-molecular-weight gaseous products generated during coal pyrolysis.

**Table 4:** Changes in the Distribution of Carbon Atoms in Pyrolysis Tar.

| Sample | Number of carbon atoms | | |
|---|---|---|---|
| | $C_6$-$C_{10}$ | $C_{11}$-$C_{19}$ | $C_{20+}$ |
| Coal | 44.61 | 32.75 | 13.59 |
| Oil | 15.17 | 39.82 | 36.07 |
| Coal + Oil (20/80) | 13.53 | 43.27 | 39.12 |
| Theoretical value | 21.06 | 38.41 | 31.57 |

### 3.4 FTIR analysis results for the semi-coke

Fig. 5 presents the FT-IR spectra of solid semi-coke obtained from the pyrolysis of coal, oil, and coal–oil mixtures with varying oil additions. Five prominent absorption peaks were observed at 1002–1015 $cm^{-1}$, 1421–1456 $cm^{-1}$, 1595–1607 $cm^{-1}$, 2920–2976 $cm^{-1}$, and 3661–3669 $cm^{-1}$. The shifts in

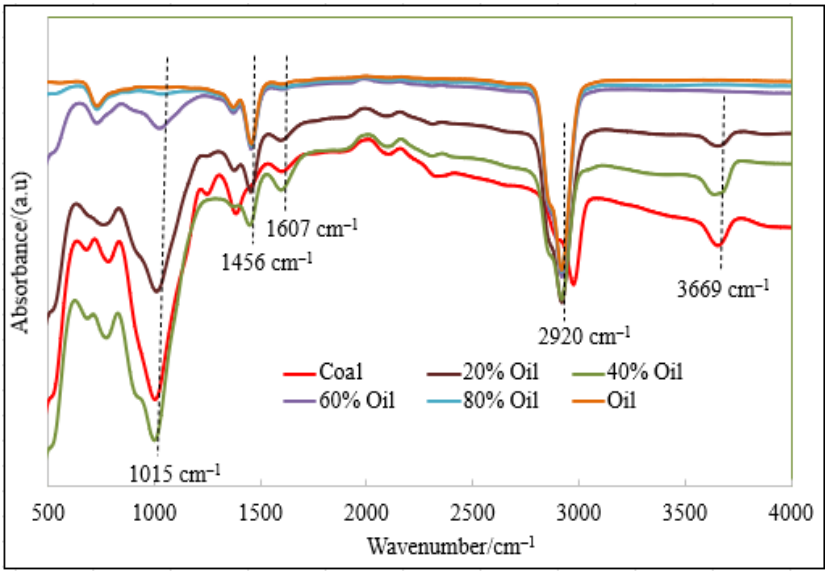


**Fig. 5:** FT-IR Spectra of Semi-Coke Samples.

these peaks due to oil addition may be attributed to changes in the organic structure, which is closely related to functional groups that induce inductive or hydrogen-bonding effects.[35]

The most intense absorption peaks were observed in the regions of 1002–1015 $cm^{-1}$ and 2920–2976 $cm^{-1}$, corresponding to out-of-plane C–O bending vibrations and antisymmetric stretching vibrations of –$CH_2$– groups, respectively.

The peaks at 1002–1015 $cm^{-1}$ indicate the presence of esters and epoxide compounds on the surface of the char. However, with the addition of oil at 60% and above, the intensity of this peak significantly decreased, which may be due to the supply of sufficient hydrogen from the oil, causing the epoxide compounds to crack and form hydrocarbon gases.[40] In the oil itself, C–O vibrations were no longer present, which were destroyed during pyrolysis. The intensities of the peaks at 2920–2976 $cm^{-1}$ (asymmetric stretching vibrations of –$CH_2$–) clearly did not change, nor did the intensities of the peaks at 1421–1456 $cm^{-1}$, which correspond to the bending vibrations of –$CH_2$–. This indicates that the addition of oil does not significantly affect the formation of aliphatic hydrocarbons. The low-intensity peaks at 1595–1607 $cm^{-1}$ correspond to the stretching vibrations of carbonyl groups C=O, but again, with the addition of oil at 60% and above (as in the case of the peaks at 1002–1015 $cm^{-1}$), the intensity of the peaks significantly decreased almost to zero, indicating a substantial reduction of carboxylic, aldehyde, and ketone groups on the surface of the semi-coke. The peaks at 3661–3669 $cm^{-1}$ correspond to the stretching vibration of hydroxyl (–OH), indicating the formation of such groups as carboxylic acids, phenols, and alcohols. However, as in the previous cases, the addition of oil at 60% led to the complete destruction of these groups. Thus, high oil addition (60% and above) leads to a significant reduction in oxygen-containing functional groups on the surface of the semi-coke. This may be due to the following factors: an increase in radicals from the oil promotes the thermal removal of oxygen in the form of $H_2O$, CO, and $CO_2$ through dehydration, decarboxylation, and decarbonylation reactions; the breaking of C–O bonds under the influence of hydrogen and hydrocarbon radicals (formed from the oil); the formation of a more stable aromatic structure of the semi-coke, which prevents the fixation of oxygen groups; heavy oil contains many asphaltenes and resins, condensed polycyclic hydrocarbons, which upon heating transition into more stable oxygen-free structures, suppressing the formation of new oxygen-containing functional groups.

### 3.5 Results of the component analysis of pyrolysis gas

The results of the pyrolysis gas analysis are presented in Table 5, from which it is evident that co-pyrolysis of coal and oil leads to an increase in the concentrations of $H_2$, $CH_4$, and $C_nH_m$, while the concentrations of CO and $CO_2$ decrease.

The increased formation of $H_2$ and $CH_4$ may be attributed to the fact that, during coal pyrolysis, a carbon-rich solid residue known as semi-coke is produced, which can act as a catalyst for the dehydrogenation and cracking of oil. This may also lead to a reduction in CO formation, as semi-coke can interact with or capture oxygen-containing species. Moreover, radicals originating from the coal matrix may further promote the cracking of oil-derived hydrocarbons, thereby increasing the yield of light hydrocarbons ($C_nH_m$) in the pyrolysis gas.

**Table 5:** Component Composition of Pyrolysis Gas.

| Sample | Component Composition | | | | |
|---|---|---|---|---|---|
| | CO, % | $H_2$, % | $CH_4$, % | $CO_2$, % | $C_nH_m$, % |
| Coal | 27.64 | 23.41 | 10.34 | 20.31 | 1.53 |
| Oil | 13.37 | 38.53 | 21.29 | 8.84 | 5.07 |
| Coal + oil (20/80) | 10.69 | 45.57 | 26.95 | 4.81 | 6.93 |

The observed decrease in CO and $CO_2$ content may also result from the fact that, during standalone coal pyrolysis,

oxygen-containing functional groups (*e.g.* carboxylic, carbonyl, and phenolic groups) decompose to form CO and $CO_2$. However, during co-pyrolysis, the oil releases a significant amount of hydrogen, which reacts with these oxygenated groups in coal, promoting hydrogenolysis. As a result, $CH_4$ and $H_2O$ are formed instead of CO and $CO_2$.

## 4. Conclusion

As a result of the conducted study on the co-pyrolysis of low-rank coal with heavy oil at various mixing ratios, the following conclusions can be drawn:

1. The addition of high-viscosity oil in the range of 20–80% significantly enhanced the co-pyrolysis process, leading to a substantial increase in tar yield from 16.34% to 67.03%. A gradual increase in pyrolysis gas yield was also observed—from 6.15% to 16.54%—while the yield of semi-coke markedly decreased from 77.51% to 16.43%. This increase in product yield is mainly attributed tothe high content of resins and asphaltenes in the heavy oil.
2. Thermal analysis via TG-DTG-DSC revealed three major decomposition stages for coal, with characteristic temperature peaks at 90.06 °C, 506.83 °C, and 712.84 °C. The addition of 20% oil resulted in the broadening of the low-temperature peak and the appearance of an additional peak at 270–299 °C, whose intensity increased with further oil addition. As the co-pyrolysis temperature rose, the second stage (peak at 507–443 °C) and third stage (peak at 713–666 °C) became evident. However, at oil additions of 60–100%, these decomposition peaks disappeared, indicating that most volatile compounds were released before reaching $T_{2max}$ and $T_{3max}$. This is likely due to the strong interaction between free radical fragments derived from both coal and oil, accelerating decomposition.
3. Both the reactor experiments and TG-DTG-DSC thermal analysis confirmed a pronounced positive synergistic effect at the coal/oil ratio of 20/80(%). At this ratio, maximum mass loss and increased $DTG_{max}$ values were observed. Furthermore, only under this condition did the experimental yields of tar and gas exceed the theoretical values (Fig. 1), and the experimental TG-DTG curves were located below the theoretical TG-DTG curves (Fig. 3). This behaviour is attributed to the significant differences in the physicochemical properties of low-rank coal and heavy oil.
4. GC–MS analysis of the pyrolysis tar from the coal–oil mixture demonstrated a substantial increase in aromatic hydrocarbons and a reduction in alkanes, olefins, and phenols. Simultaneously, gas composition analysis revealed an increase in the concentrations of $H_2$, $CH_4$, and $C_nH_m$, along with a decrease in CO and $CO_2$, due to the presence of oil in the system.
5. The results of this study demonstrate the feasibility and effectiveness of the co-pyrolysis of low-rank coal with heavy oil for the production of high value-added products. This addresses one of the key challenges in the energy sector and presents an approach with considerable potential for the development of efficient and environmentally sustainable technologies for processing both low-grade and unconventional hydrocarbon feedstocks. The methodology not only enhances product yields but also improves product quality and overall process efficiency.
6. Moreover, as previously mentioned, the coal and oil feedstocks used in this study exhibit contrasting chemical and physical properties (such as proximate and ultimate composition, H/C ratio, density, viscosity, thermal conductivity, etc.), which contributed to the pronounced synergistic effect observed. Therefore, the results of this study—including the co-pyrolysis method—can be applied not only to other similar feedstocks (even those with characteristics different from those used here), but also to other types of raw materials, such as plastic and rubber waste, oil shale, biomass, and other organo-mineral materials. Thus, a key condition for enhancing the efficiency and optimizing the co-pyrolysis process is a significant difference in the physicochemical properties of the feedstock components. Furthermore, co-pyrolysis of mixtures containing more than two types of feedstocks is of particular interest, as it not only promotes more complete interaction between components, but also expands the range of usable raw materials and increases the flexibility of the technology.

## Acknowledgments

This work was carried out with financial support from the Science Committee of the Ministry of Science and Higher Education of the Republic of Kazakhstan (No. BR21882171 "SDG 9.4: Development of the "green" economy of Kazakhstan through the processing of mineral raw materials and waste by pyrolysis").

## Conflict of Interest

The authors declare that they have no known competing financial interests or personal relationships that could have appeared to influence the work reported in this paper.

## Supporting Information

Not applicable.

## CRediT Statement

**N. U. Nurgaliyev:** Conceptualization, Supervision, Writing – review & editing. **Ye. K. Aibuldinov:** Conceptualization, Methodology, Project administration. **E. E. Kopishev:** Supervision, Writing – review & editing. **Zh. B. Iskakova:** Data curation, Investigation. **A. Kolpek:** Formal analysis, Visualization. Sabitov A.S.: Writing – original draft, Data

curation, Formal analysis. **L. A. Kusepova:** Resources, Investigation. **R. M. Salikhov:** Software, Validation. **M. S. Petrov:** Investigation, Methodology. Corresponding authors: **N. U. Nurgaliyev** and **A. S. Sabitov**

## References


[1] Garside M, Global proven coal reserves by country 2020, Online available: https://www.statista.com/statistics/237096/proven-coal-reserves-of-the-top-ten-countries.

[2] H. Katalambula and R. Gupta, Low-grade coals: a review of some prospective upgrading technologies, *Energy & Fuels*, 2009, **23**, 3392-3405, doi: 10.1021/ef801140t.

[3] J. Zhou, L. Wu, K. Liang, J. Zhou, Q. Zhang, Y. Song, Y. Tian, X. Lan, Spectroscopic analysis of products from low-rank coal microwave pyrolysis : effect of reaction atmosphere, *Journal of Applied Spectroscopy*, 2020, **87**, 745-752, doi: 10.1007/s10812-020-01064-5.

[4] Y. Liu, Q. Yao, M. Sun, X. Ma, Catalytic fast pyrolysis of coal tar asphaltene over zeolite catalysts to produce high-grade coal tar: an analytical Py-GC/MS study, *Journal of Analytical and Applied Pyrolysis*, 2021, **156**, 105127, doi: 10.1016/j.jaap.2021.105127.

[5] Y. Che, K. Shi, Z. Cui, H. Liu, Q. Wang, W. Zhu, Y. Tian, Conversion of low temperature coal tar into high value-added chemicals based on the coupling process of fast pyrolysis and catalytic cracking, *Energy*, 2023, **264**, 126169, doi: 10.1016/j.energy.2022.126169.

[6] Z.-H. Ma, X.-Y. Wei, G.-H. Liu, F.-J. Liu, Z.-M. Zong, Value-added utilization of high-temperature coal tar: a review, *Fuel*, 2021, **292**, 119954, doi: 10.1016/j.fuel.2020.119954.

[7] N. Liu, H. Huang, X. Huang, R. Li, J. Feng, Y. Wu, Co-pyrolysis Behavior of Coal and Biomass: Synergistic Effect and Kinetic Analysis. *ACS Omega*, 2024, **9**(29), 31803-31813, doi.10.1021/acsomega.4c03053.

[8] Q. Zhang, S. Zhang, J. Liu, J. Li, J. Liu, J. Zhou, L. Wu, Catalytic upgrading of volatiles in co-pyrolysis of coal and biomass by Mo-MFI molecular sieves, *RSC Advances*, 2023, **13**, 33852-33862, doi: 10.1039/d3ra06925g.

[9] B. Wang, N. Liu, S. Wang, X. Li, R. Li, Y. Wu, Study on co-pyrolysis of coal and biomass and process simulation optimization, *Sustainability*, 2023, **15**, 15412, doi: 10.3390/su152115412.

[10] S. M. Gouws, M. Carrier, J. R. Bunt, H. W. J. P. Neomagus, Co-pyrolysis of coal and raw/torrefied biomass: a review on chemistry, kinetics and implementation, *Renewable and Sustainable Energy Reviews*, 2021, **135**, 110189, doi: 10.1016/j.rser.2020.110189.

[11] A. O. Aboyade, M. Carrier, E. L. Meyer, H. Knoetze, J. F. Görgens, Slow and pressurized co-pyrolysis of coal and agricultural residues, *Energy Conversion and Management*, 2013, **65**, 198-207, doi: 10.1016/j.enconman.2012.08.006.

[12] S. Saeed, M. Saleem, A. Durrani, Thermal performance analysis and synergistic effect on co-pyrolysis of coal and sugarcane bagasse blends pretreated by trihexyltetradecylphosphonium chloride, *Fuel*, 2020, **278**, 118240, doi: 10.1016/j.fuel.2020.118240.

[13] R. Jelita, I. F. Nata, C. Irawan, J. Jefriadi, M. Hafiz, I. Angreini, M. D. Putra, Characterization and comparative study of pyrolysis of low rank coal and biomass, *Journal of Chemical Technology and Metallurgy*, 2024, **59**, 73-80, doi: 10.59957/jctm.v59.i1.2024.8.

[14] Z. Brat, B. Jankovic, D. Stojiljkovic, M. Radojevic, N. Manic, Assessment of synergistic effect on performing the co-pyrolysis process of coal and waste blends based on thermal analysis, *Thermal Science*, 2022, **26**, 2211-2224, doi: 10.2298/tsci210516310b.

[15] P. Zhang, Z. Chen, Q. Zhang, S. Zhang, X. Ning, J. Zhou, Co-pyrolysis characteristics and kinetics of low metamorphic coal and pine sawdust, *RSC Advances*, 2022, **12**, 21725-21735, doi: 10.1039/d2ra02461f.

[16] Z. Wu, W. Yang, X. Tian, B. Yang, Synergistic effects from co-pyrolysis of low-rank coal and model components of microalgae biomass, *Energy Conversion and Management*, 2017, **135**, 212-225, doi: 10.1016/j.enconman.2016.12.060.

[17] Y. Huang, N. Wang, Q. Liu, W. Wang, X. Ma, Co-pyrolysis of bituminous coal and biomass in a pressured fluidized bed, *Chinese Journal of Chemical Engineering*, 2019, **38**(7), 1666-1673.

[18] W. Feng, M. Zheng, L. Jin, J. Bai, L. Kong, H. Li, Z. Bai, W. Li, Co-pyrolysis behaviors of coal and polyethylene by combining *in situ* Py-TOF-MS and reactive molecular dynamics, *Fuel*, 2023, **331**, 125802, doi: 10.1016/j.fuel.2022.125802.

[19] A. Khan, N. Iqbal, T. Noor, M. Hassan, J. Akhter, Synergistic production of fuels from co-pyrolysis of lignite coal and waste plastic, *Journal of the Energy Institute*, 2024, **113**, 101527, doi: 10.1016/j.joei.2024.101527.

[20] A. Khan, N. Iqbal, T. Noor, A. Iqtidar, N. Khan, Pyrolysis of lignite coal and waste tires for liquid fuel production, *Journal of the Energy Institute*, 2025, **120**, 102065, doi: 10.1016/j.joei.2025.102065.

[21] O. Bičáková, P. Straka, Co-pyrolysis of waste tire/coal mixtures for smokeless fuel, maltenes and hydrogen-rich gas production, *Energy Conversion and Management*, 2016, **116**, 203-213, doi: 10.1016/j.enconman.2016.02.069.

[22] F. Mushtaq, R. Mat, F. N. Ani, A review on microwave assisted pyrolysis of coal and biomass for fuel production, *Renewable and Sustainable Energy Reviews*, 2014, **39**, 555-574,

doi: 10.1016/j.rser.2014.07.073.
[23] X. Chen, L. Liu, L. Zhang, Y. Zhao, P. Qiu, R. Ruan, A review on the properties of copyrolysis char from coal blended with biomass, *Energy & Fuels*, 2020, **34**, 3996-4005, doi: 10.1021/acs.energyfuels.0c00014.
[24] G. Hu, J. Li, X. Zhang, Y. Li, Investigation of waste biomass co-pyrolysis with petroleum sludge using a response surface methodology, *Journal of Environmental Management*, 2017, **192**, 234-242, doi: 10.1016/j.jenvman.2017.01.069.
[25] R. M. Soncini, N. C. Means, N. T. Weiland, Co-pyrolysis of low rank coals and biomass: Product distributions, *Fuel*, 2013, **112**, 74-82, doi: 10.1016/j.fuel.2013.04.073.
[26] N. Yin, Y. Song, L. Wu, P. Dong, C. Wang, J. Zhou, X. Zhang, Analysis of tar and pyrolysis gas from low-rank coal pyrolysis assisted by apple branch, *Journal of Renewable and Sustainable Energy*, 2023, **15**, 043102, doi: 10.1063/5.0156660.
[27] Y. Li, S. Huang, Q. Wang, H. Li, Q. Zhang, H. Wang, Y. Wu, S. Wu, J. Gao, Hydrogen transfer route and interaction mechanism during co-pyrolysis of Xilinhot lignite and rice husk, *Fuel Processing Technology*, 2019, **192**, 13-20, doi: 10.1016/j.fuproc.2019.04.022.
[28] Y. Huang, N. Wang, Q. Liu, W. Wang, X. Ma, Co-pyrolysis of bituminous coal and biomass in a pressured fluidized bed, *Chinese Journal of Chemical Engineering*, 2019, **38**(7), 1666-1673.
[29] Y. Song, N. Yin, D. Yao, Q. Ma, J. Zhou, X. Lan, Co-pyrolysis characteristics and synergistic mechanism of low-rank coal and direct liquefaction residue, *Energy Sources, Part A: Recovery, Utilization, and Environmental Effects*, 2019, **41**, 2675-2689, doi: 10.1080/15567036.2019.1568639.
[30] J. Xu, Z. Bai, J. Bai, L. Kong, D. Lv, Y. Han, X. Dai, W. Li, Physico-chemical structure and combustion properties of chars derived from co-pyrolysis of lignite with direct coal liquefaction residue, *Fuel*, 2017, **187**, 103-110, doi: 10.1016/j.fuel.2016.09.028.
[31] N. Yin, Y. H. Song, J. Zhou, Y. H. Tian, A. W. Yang, Effects of direct coal liquefaction residue additions on low-rank pulverized coal during co-pyrolysis, *Materials Science Forum*, 2020, **999**, 167-177, doi: 10.4028/www.scientific.net/msf.999.167.
[32] T. Su, Y. Song, X. Lan, Product characteristics and interaction mechanism in low-rank coal and coking coal co-pyrolysis process, *Journal of Chemical Engineering of Japan*, 2020, **53**, 167-176, doi: 10.1252/jcej.18we172.
[33] Z. Miao, G. Wu, P. Li, X. Meng, Z. Zheng, Investigation into co-pyrolysis characteristics of oil shale and coal, *International Journal of Mining Science and Technology*, 2012, **22**, 245-249, doi: 10.1016/j.ijmst.2011.09.003.
[34] B. T. Yermagambet, Zh. M. Kassenova, N. U. Nurgaliyev, M. K. Kazankapova, S. M. Martemyanov, Calculation of Kinetic Parameters of Thermal Decomposition of Coals of Various Deposits of Kazakhstan, *News of the Academy of Sciences of the Republic of Kazakhstan*, Series of Geology and Technical Sciences, 2020, **442**, 86-93, doi.10.32014/2020.2518-170X.88.
[35] Y. Song, N. Yin, D. Yao, Q. Ma, J. Zhou, X. Lan, Co-pyrolysis characteristics and synergistic mechanism of low-rank coal and direct liquefaction residue, *Energy Sources, Part A: Recovery, Utilization, and Environmental Effects*, 2019, **41**, 2675-2689, doi: 10.1080/15567036.2019.1568639.
[36] Y. Li, S. Huang, Q. Wang, H. Li, Q. Zhang, H. Wang, Y. Wu, S. Wu, J. Gao, Hydrogen transfer route and interaction mechanism during co-pyrolysis of Xilinhot lignite and rice husk, *Fuel Processing Technology*, 2019, **192**, 13-20, doi: 10.1016/j.fuproc.2019.04.022.
[37] W. Feng, M. Zheng, L. Jin, J. Bai, L. Kong, H. Li, Z. Bai, W. Li, Co-pyrolysis behaviors of coal and polyethylene by combining *in situ* Py-TOF-MS and reactive molecular dynamics, *Fuel*, 2023, **331**, 125802, doi: 10.1016/j.fuel.2022.125802.
[38] Y.-H. Song, Q.-N. Ma, W.-J. He, Co-pyrolysis properties and product composition of low-rank coal and heavy oil, *Energy & Fuels*, 2017, **31**, 217-223, doi: 10.1021/acs.energyfuels.6b02106.
[39] B. Lin, Q. Huang, Y. Chi, Co-pyrolysis of oily sludge and rice husk for improving pyrolysis oil quality, *Fuel Processing Technology*, 2018, **177**, 275-282, doi: 10.1016/j.fuproc.2018.05.002.
[40] N. Yin, Y. H. Song, J. Zhou, Y. H. Tian, A. W. Yang, Effects of Direct Coal Liquefaction Residue Additions on Low-Rank Pulverized Coal During Co-Pyrolysis. *Materials Science Forum*, Publisher in materials and engineering, 2020, **999**, 167-177, doi. 10.4028/www.scientific.net/MSF.999.167.
[41] N. Liu, H. Huang, X. Huang, R. Li, J. Feng, Y. Wu, Co-pyrolysis Behavior of Coal and Biomass: Synergistic Effect and Kinetic Analysis, *ACS Omega*, 2024, **9**(29), 31803-31813, doi.10.1021/acsomega.4c03053.